Cross-sections of e^+e^- annihilation into open or hidden charm states


Vladimir Khachatryan

Hadronic Physics Group
Department of Physics, Indiana University

BEACH 2024: XV International Conference on Beauty, Charm, Hyperons in Hadronic Interactions

June 3-7 2024, Charleston, South Carolina, USA

Outline

- General introduction on open/hidden charm states, and on BESIII apparatus/analysis

- Representing main results of BESIII three recent papers

1) arXiv:2403.14998 [hep-ex]
Precise measurement of the $e^+e^- \to D_s^+D_s^-$ cross sections at center-of-mass energies from threshold to 4.95 GeV,

2) arXiv:2402.03829 [hep-ex]
Precise Measurement of Born Cross Sections for $e^+e^- \to D\bar{D}$ and Observation of One Structure between $\sqrt{s}$ = 3.80 - 4.95 GeV,

3) Phys. Rev. D 109, 092012 (2024), arXiv:2310.03361 [hep-ex]
Measurement of $e^+e^- \to \eta J/\psi$ Cross Section from $\sqrt{s}$ = 3.808 GeV to 4.951 GeV,

- Summary

- Over past decades many charmonium-like states discovered: $J^{PC} = 1^{--}$
- Conventional charmonium states (ψ(3770), ψ(4040), ψ(4160), ψ(4415)) decaying to open-charm final states, such as $D^*\bar{D}^*$, etc.
- Y states showing strong coupling to hidden-charm final states, such as $\pi^+\pi^- J/\psi$
- Above-mentioned features suggesting that perhaps the Y states not to be conventional charmonia
  - Exotic composition most likely required
  - Good candidates for hybrids, tetraquarks, and mesonic molecules

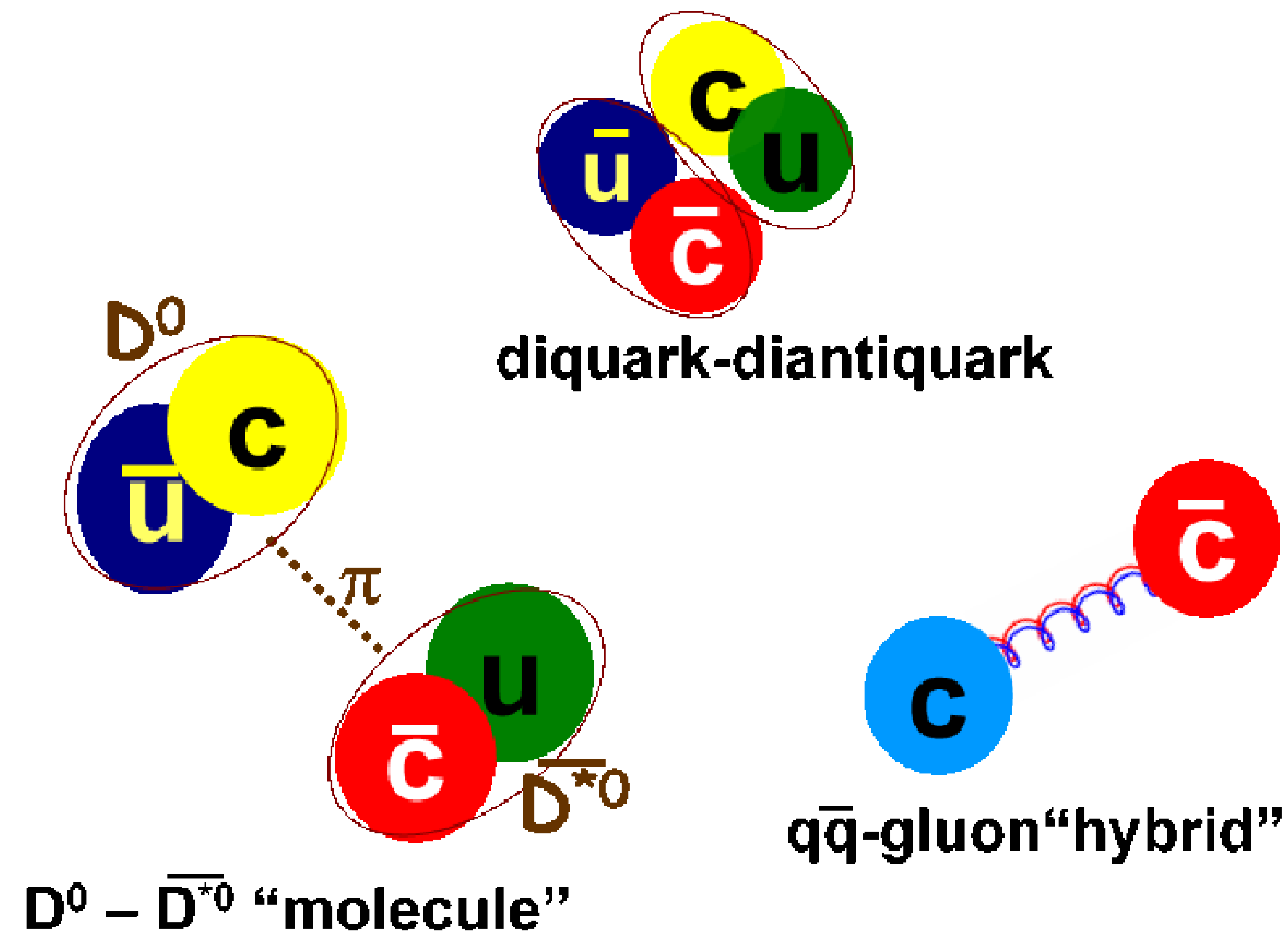

- Y(4260), Y(4360), and Y(4660) considered to be exotic candidates
  - Currently designated as ψ(4230), ψ(4360), and ψ(4660)
- Precise measurements of production cross sections and resonance parameters needed
  - to clarify nature of these states
  - to distinguish among different theoretical models

- General-purpose detector BESIII
  Nucl. Instrum. Meth. A 614, 345 (2010)
- Located at the Beijing Electron Positron Collider (BEPCII)
- Started in summer 2008 and has run at multiple energies
- Operating at peak luminosity at 10^{33} cm^{-2} s^{-1}
- Given the center-of-mass energy range from 2.0 to 4.95 GeV
- Detector recording symmetric e^+e^- collisions provided by the BEPCII storage ring
- Designed for studies of hadron spectroscopy and τ - charm physics

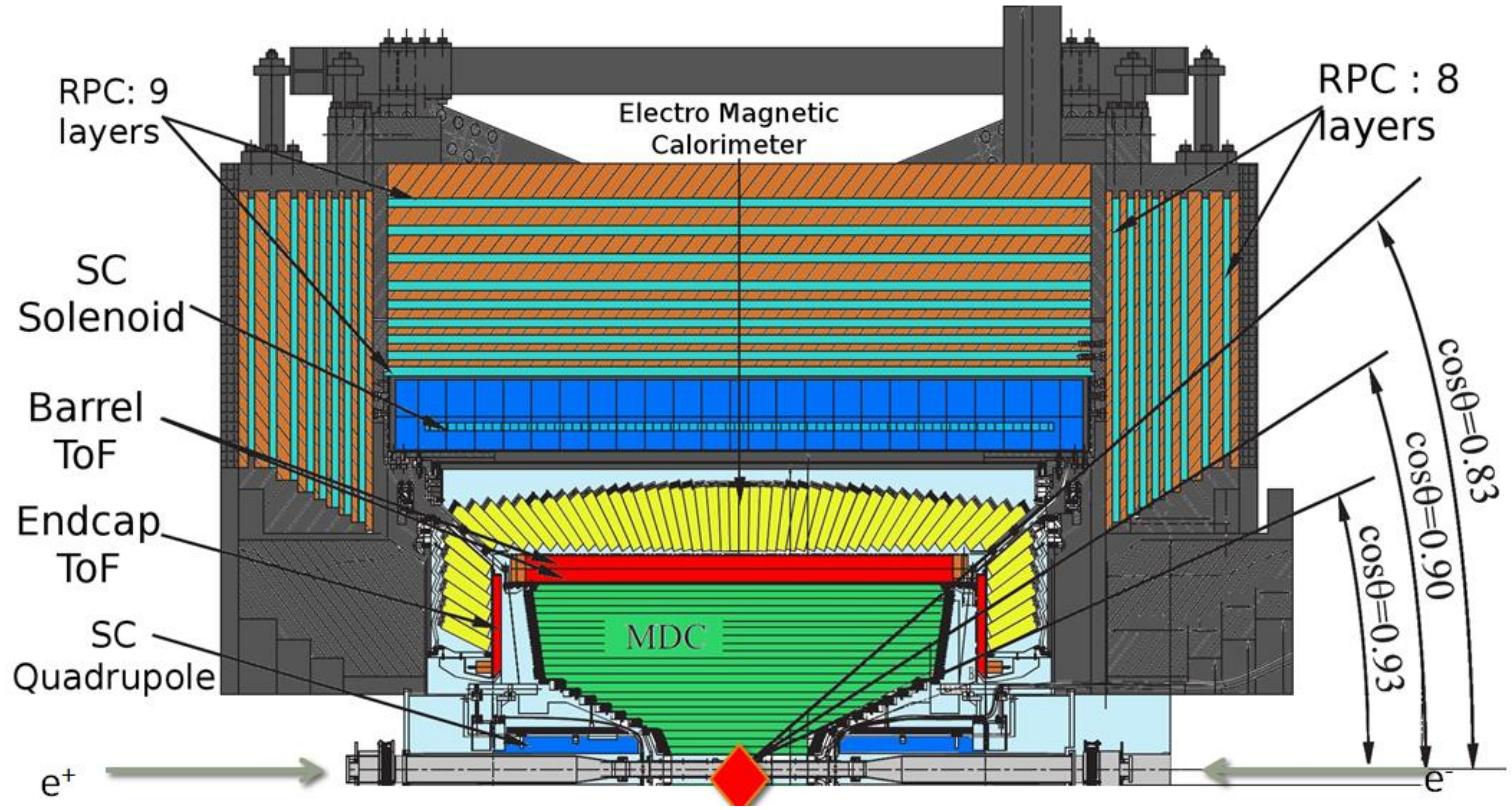

Motivation

- Masses of $\psi(4230)$, $\psi(4360)$, and $\psi(4660)$ lie above open-charm threshold
  - Measurement of their couplings to open-charm channels crucial for understanding of their nature
- Such studies being very complicated due to presence of coupled-channel effects
- Knowledge of exclusive open-charm cross sections as highly desirable
  - Such as cross section for $e^+e^- \to D_s^+ D_s^-$
- This process previously studied by Belle, BaBar, and CLEO-c
- Larger data samples collected by BESIII over a broader energy range
  - Allowing improved measurements of exclusive open-charm cross sections
- Recent publication by BESIII Phys. Rev. Lett. 131, 151903 (2023)
  - Unusual line shape observed in cross section of $e^+e^- \to D_s^{*+} D_s^{*-}$

- Cross sections measured in cm energy range between 3.94 GeV and 4.95 GeV
  - Having 138 energy points corresponding to integrated luminosity of 22.9 fb^{-1} in total
  - High-statistics XYZ data sets accounting for 95% of total integrated luminosity
  - Low-statistics R-value data sets for fine scanning, accounting for integrated luminosity around 7 pb^{-1} at each energy point

- Given low background level and high detection efficiency at BESIII
  - Only decay of $D_s^- \to K^+K^-\pi^-$ being reconstructed
  - While D_s^+ being tagged by recoil mass

- To improve signal purity, D_s^- candidates selected with two intermediate decay modes
  - $D_s^- \to \phi\,\pi^-$ with $\phi \to K^+K^-$

    or

  - $D_s^- \to K^*(892)^0 K^-$ with $K^*(892)^0 \to K^+\pi^-$

- Clear cluster of events corresponding to $D_s^+ D_s^-$ pair observed in two-dimensional plots below
- Similar signals observed in data samples at other energy points

Left plots:

Two-dimensional distributions of recoil mass of $D_s^\pm$ vs. invariant mass of combination of $K^+K^-\pi^-$

Red arrows showing signal interval

Right plots:

Red curves showing fits to distribution $M(K^+K^-\pi^-)$

Background shape shown in blue

Signal shape shown in yellow

Data points measured at
$\boldsymbol{E_{\mathrm{CM}} = 4.26\ \mathrm{GeV}}$
$\boldsymbol{E_{\mathrm{CM}} = 4.68\ \mathrm{GeV}}$

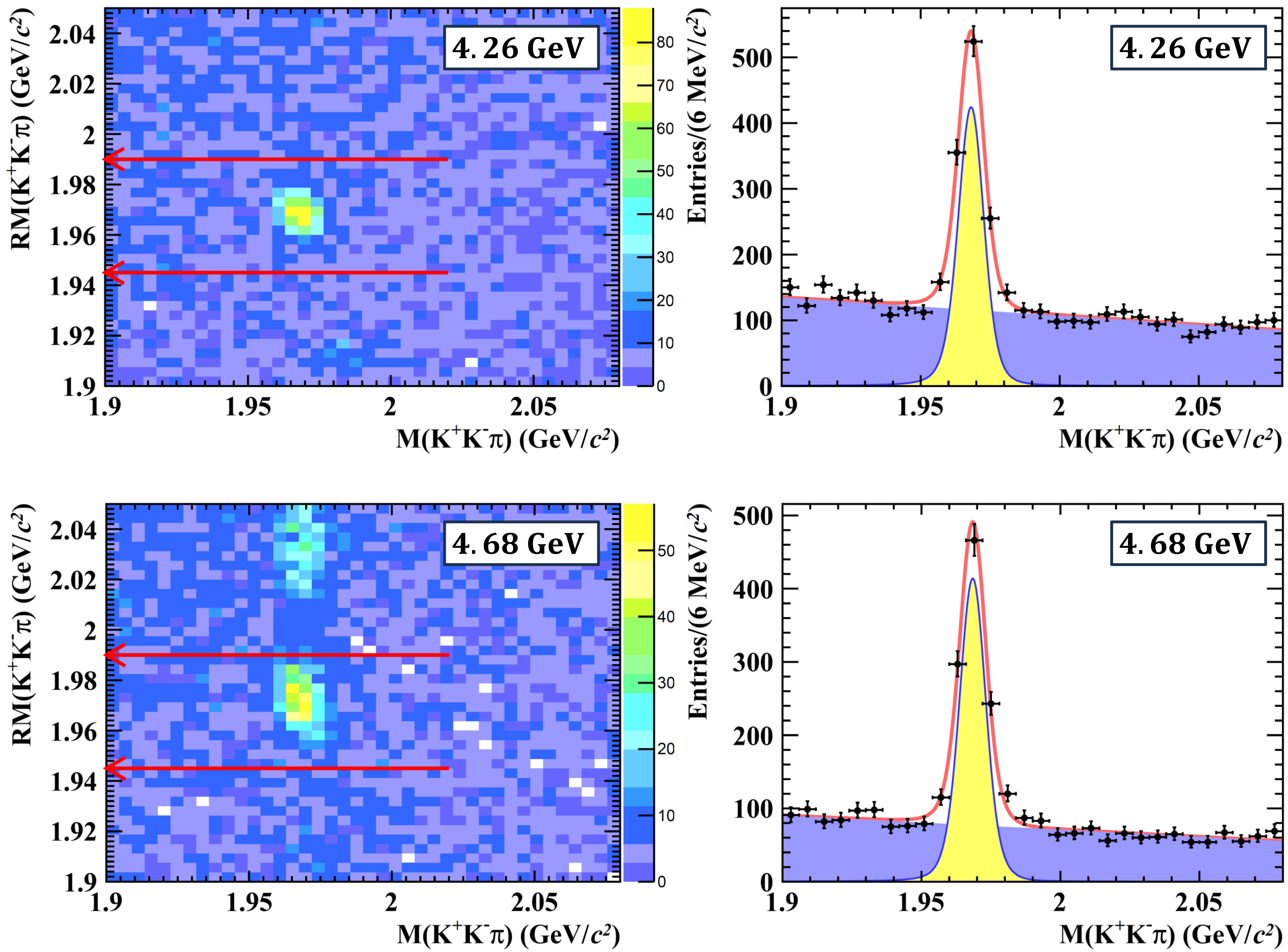

- Signal shape being described with signal MC samples convolved with Gaussian function

- Born cross section determined with

$$\sigma_{\rm Born} = \frac{N^{\rm fit}_{D_s} - N_{D_s^\pm D_s^{\mp *}}}{2\mathcal{B}(D_s^\pm \to K^+K^-\pi^\pm)\epsilon(1+\delta)\frac{1}{|1-\Pi|^2}\mathcal{L}}$$

where

- $N^{\rm fit}_{D_s}$ obtained from fitting $M(K^+K^-\pi^\pm)$ distribution in data
- $N_{D_s^\pm D_s^{\mp *}}$ describing peaking background from $e^+e^- \to D_s^+D_s^-$ (only above $E_{\rm cm}$ > 4.6 GeV)
- Factor 1/2 taking into account contributions from both D_s^+ and D_s^- single tag reconstruction
- $\mathcal{B}$ -- branching fraction of $D_s^\pm \to K^+K^-\pi^\pm$
- ϵ -- signal detection efficiency, $(1+\delta)$ -- ISR correction factor,
- $\frac{1}{|1-\Pi|^2}$ -- vacuum polarization (VP), $\mathcal{L}$ -- integrated luminosity

- As notable observation is presence of broad structure spanning from $E_{\rm cm}$ = 4.1 to 4.4 GeV
- In particular
  - Dip observed close to $D_s^{*+}D_s^{*-}$ threshold (4.224 GeV) and position of $\psi(4230)$
  - Peak observed around $\psi(4040)$

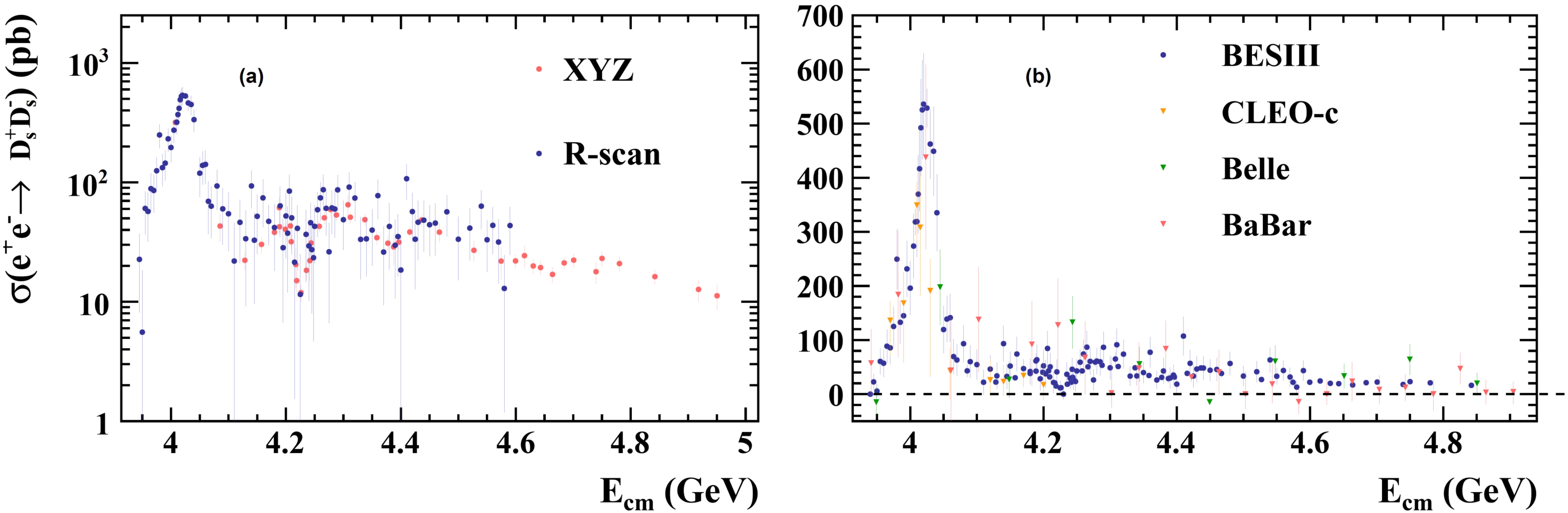

Left plot: Measured Born cross sections of $e^+e^- \to D_s^+ D_s^-$ in **log scale** as a function of energy

Right plot: Measured Born cross sections of $e^+e^- \to D_s^+ D_s^-$ in **linear scale** as a function of energy

Error bars include statistical and systematic uncertainties in quadrature

- Figures showing Born cross-section ratios
- Significantly narrower width of $\psi(4040)$ than PDG value observed
- Dip around $D_s^{*+}D_s^{*-}$ threshold and peak position of $\psi(4230)$ observed
  - Suggesting influence of open channel effect
- Two structures similar to those observed in modes of $D_s^{*+}D_s^{*-}$, K^+K^-J/ψ, $K_S^0K_S^0J/\psi$ being identified
  - Critical for understanding of non-exotic and exotic states in this energy region

$$\frac{\sigma(e^+e^- \to D_s^+D_s^-)}{\sigma(e^+e^- \to K_S^0K_S^0J/\psi)} \rightarrow$$

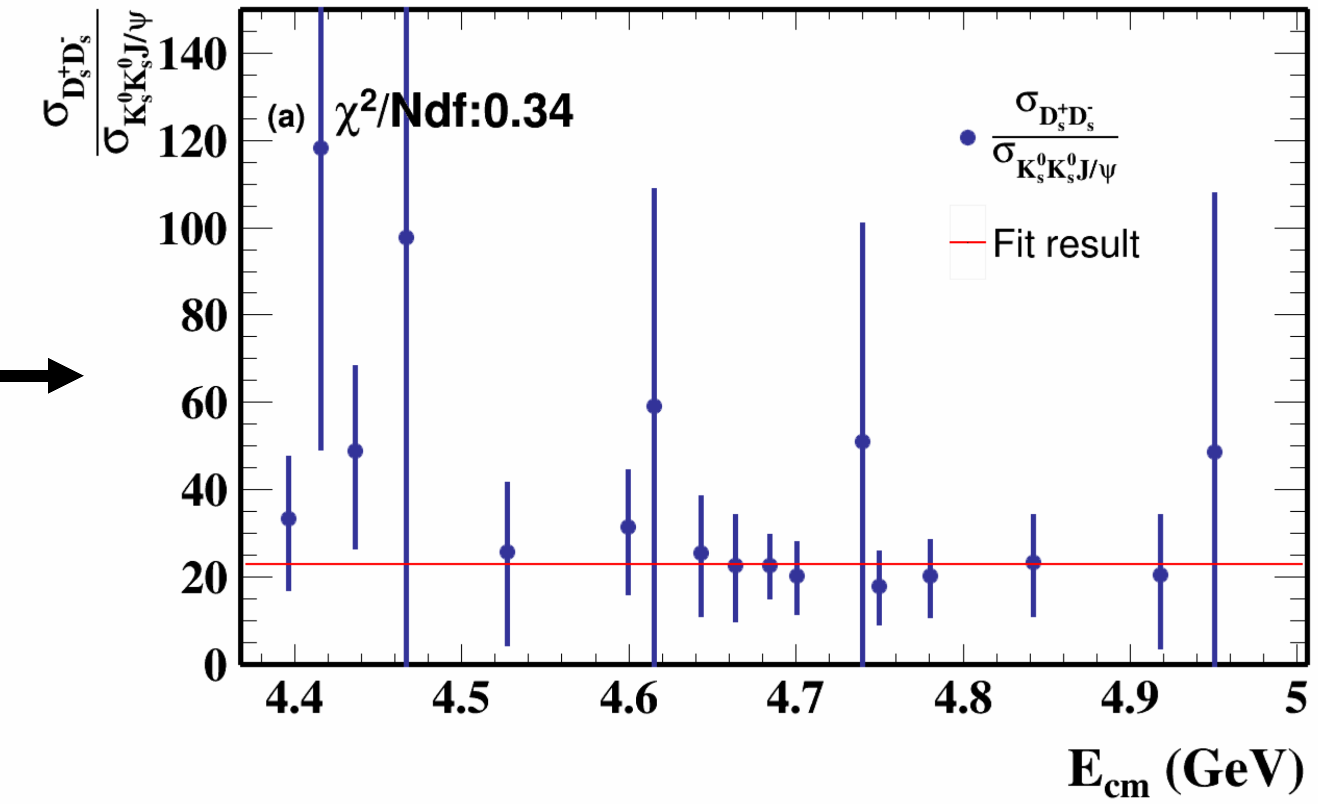

$$\frac{\sigma(e^+e^- \to D_s^+D_s^-)}{\sigma(e^+e^- \to D_s^{*+}D_s^{*-})} \rightarrow$$

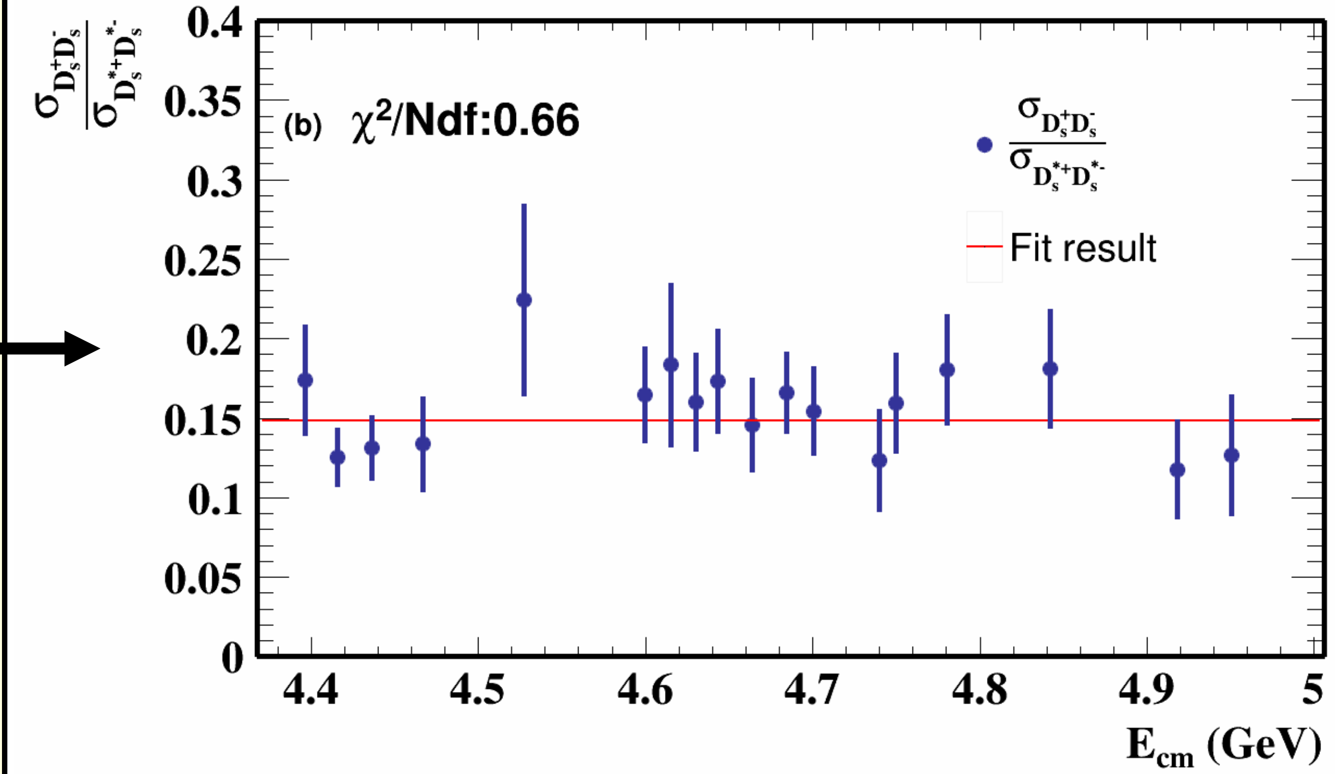

$$\frac{\sigma(e^+e^- \to D_s^+D_s^-)}{\sigma(e^+e^- \to K^+K^-J/\psi)} \rightarrow$$

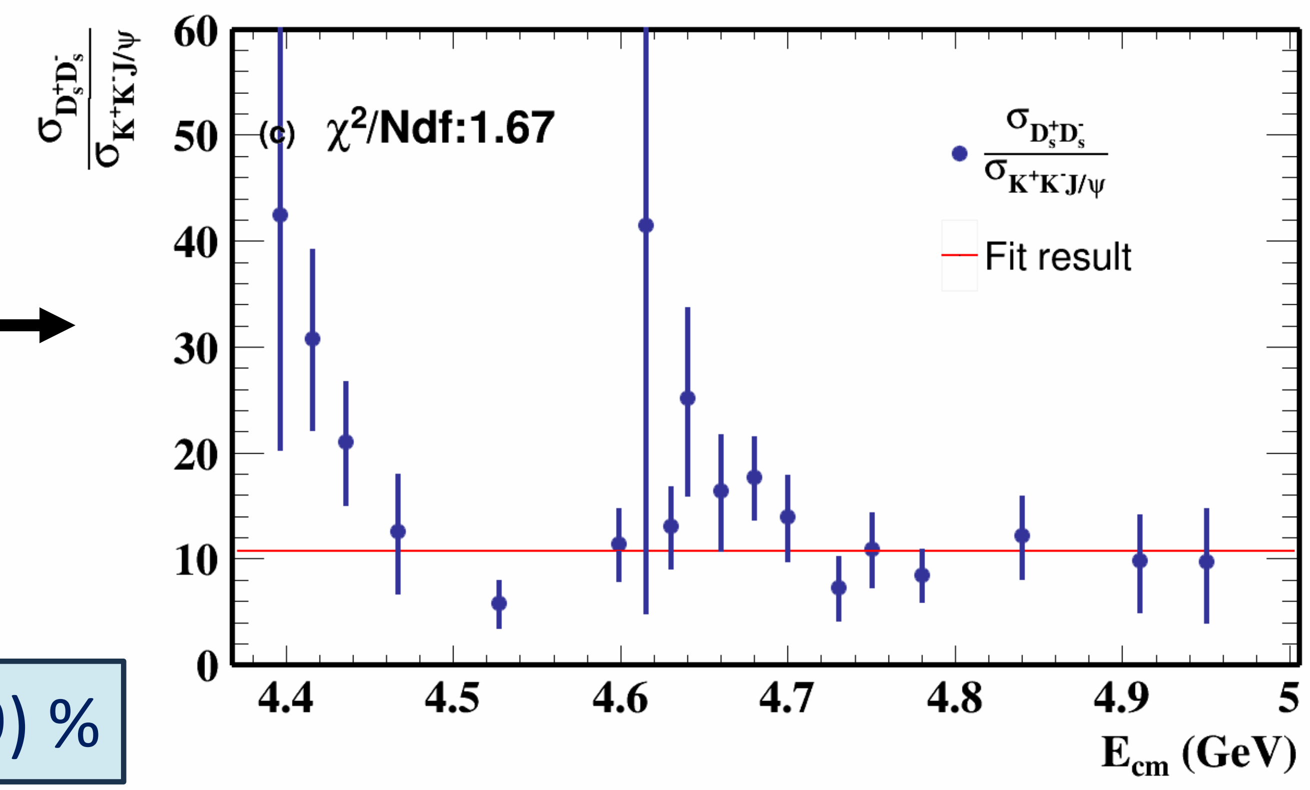

Cross-section total systematic uncertainties evaluated to be (5.6 - 6.9) %

Motivation

- Looking into other processes for studying $\psi(4230)$, $\psi(4360)$, and $\psi(4660)$
  - Such as $e^+e^- \to D^0\bar{D}^0$ and $e^+e^- \to D^+D^-$
- These states may be pure charmonium states
  - Should predominantly decay into $D\bar{D}$ final state predicted theoretically
- Currently, available observed cross sections existing for limited energy points
  - Measured by BaBar and Belle using ISR process
  - Measured by CLEO through direct e^+e^- production
- Highly desirable to precisely measure exclusive Born cross section of $e^+e^- \to D\bar{D}$ process
  - To validate interpretations of established ψ states
  - To provide additional insight into energy range above open-charm threshold

- Cross sections measured in cm energy range between 3.80 GeV and 4.95 GeV
  - Having 150 energy points corresponding to integrated luminosity of 20 fb^{-1} in total
  - With high-statistics XYZ data sample
  - With remaining low-statistics R-scan data sample

- Single tag technique employed, given purpose of achieving high efficiency for event selection
  - D^0 candidates reconstructed from $K^-\pi^+\pi^+\pi^-$
  - D^+ candidates reconstructed from $K^-\pi^+\pi^+$
  - $\bar{D}^0$ candidates inferred by mass recoiling against tagged meson (M_D^{recoil}) via $K^-\pi^+\pi^+\pi^-$ system
  - D^- candidates inferred by M_D^{recoil} via $K^-\pi^+\pi^+$ system

$$M_D^{\mathrm{recoil}} = \sqrt{(\sqrt{s} - E_D)^2 - |\mathbf{p}_D|^2}$$

with E_D and $\mathbf{p}_D$ to be energy and momentum for selected $K^-\pi^+\pi^+\pi^-$/ $K^-\pi^+\pi^+$ candidates

- Signal yields for $e^+e^- \to D\overline{D}$ process at each energy point extracted by performing (extended maximum likelihood) fit to mass recoil spectrum

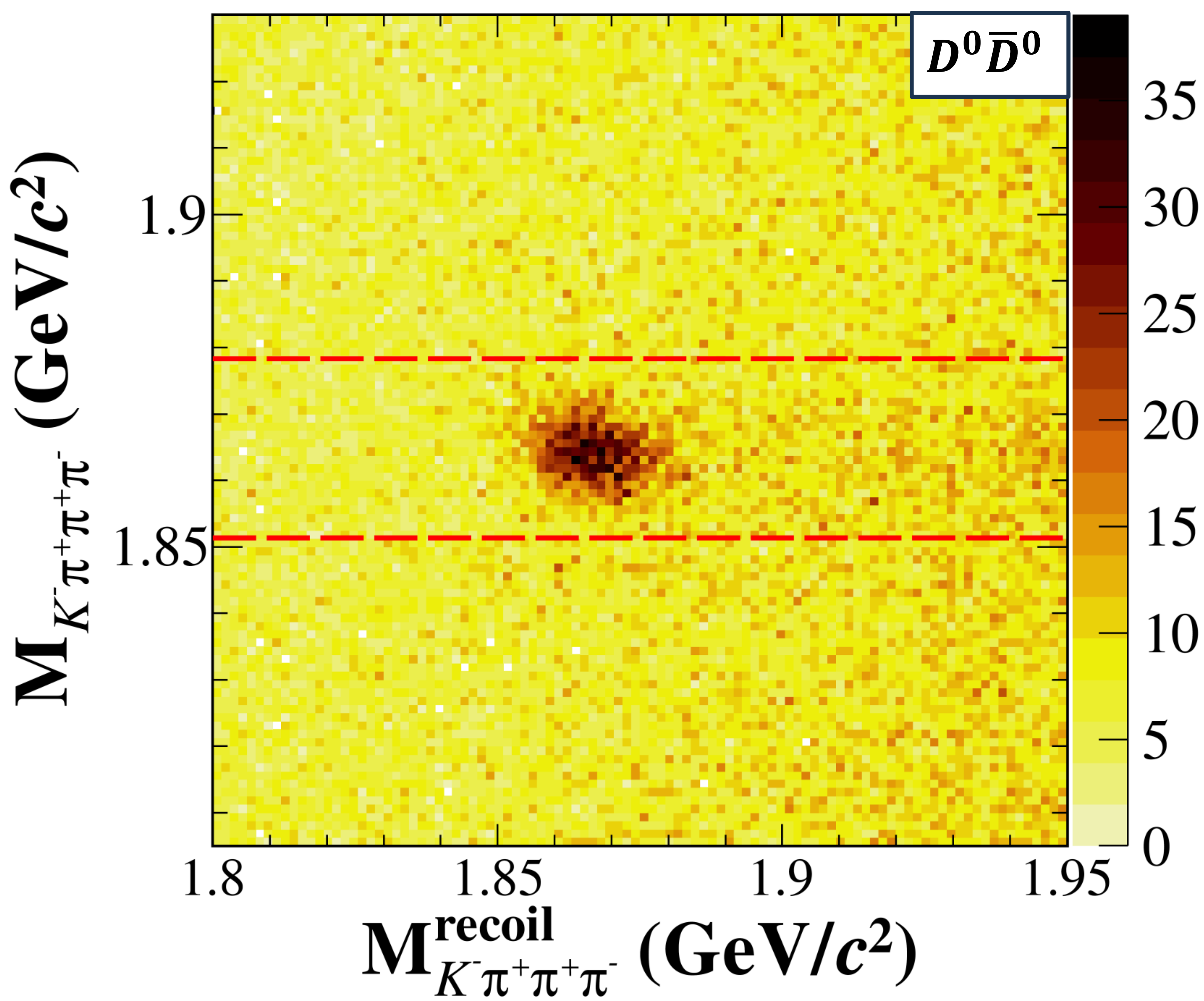

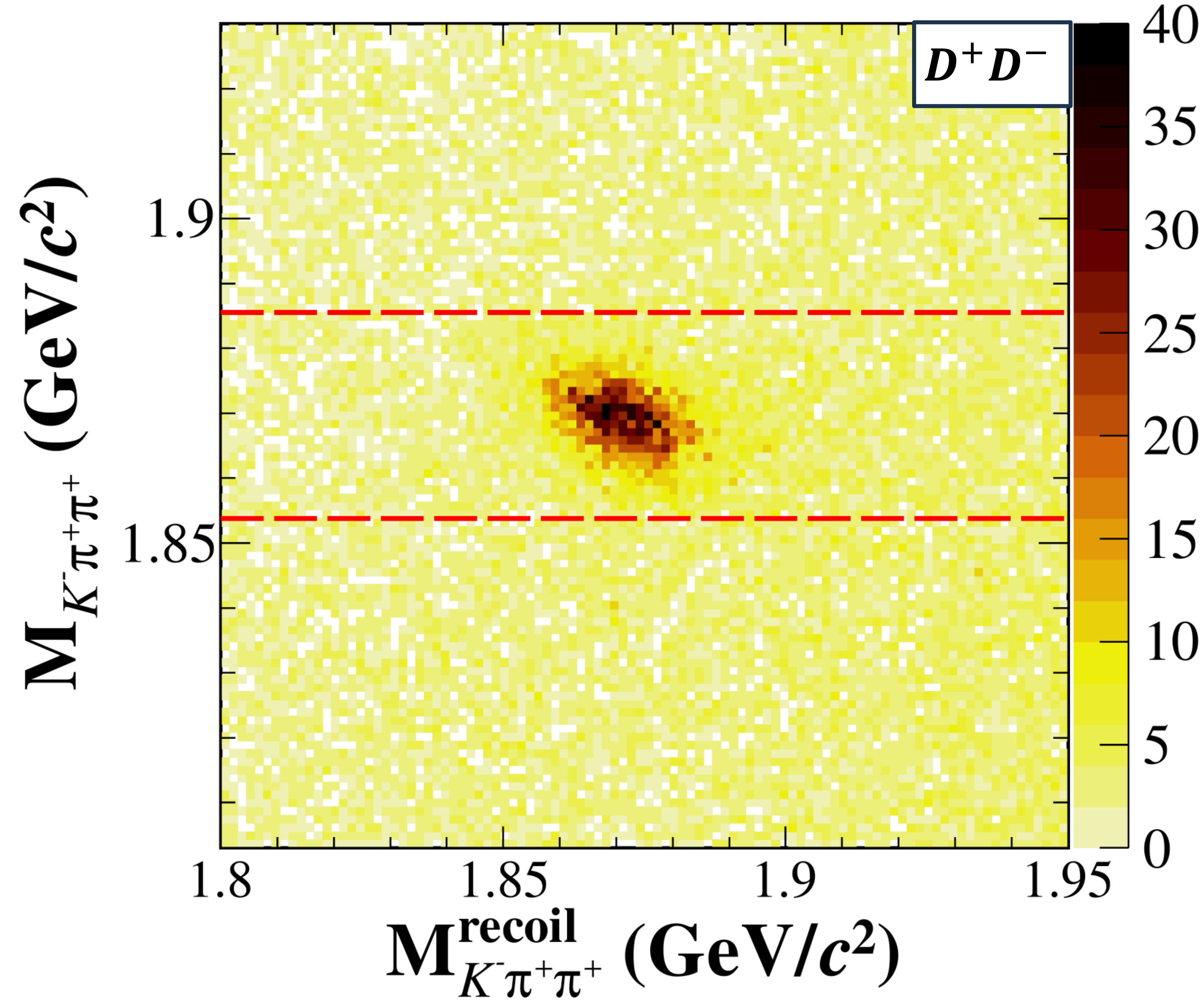

Two-dimensional distributions of invariant mass M_D vs. recoil mass M_D^{recoil} at $\sqrt{s}$ = 4.1992 GeV

Left plot: Dashed lines representing signal region for D meson in $\boldsymbol{D^0\overline{D}^0}$ **mode**

Right plot: Dashed lines representing signal region for D meson in $\boldsymbol{D^+D^-}$ **mode**

- Signal shape being described with signal MC samples convolved with Gaussian function
  - Accounting for difference in mass resolution between data and MC-simulation

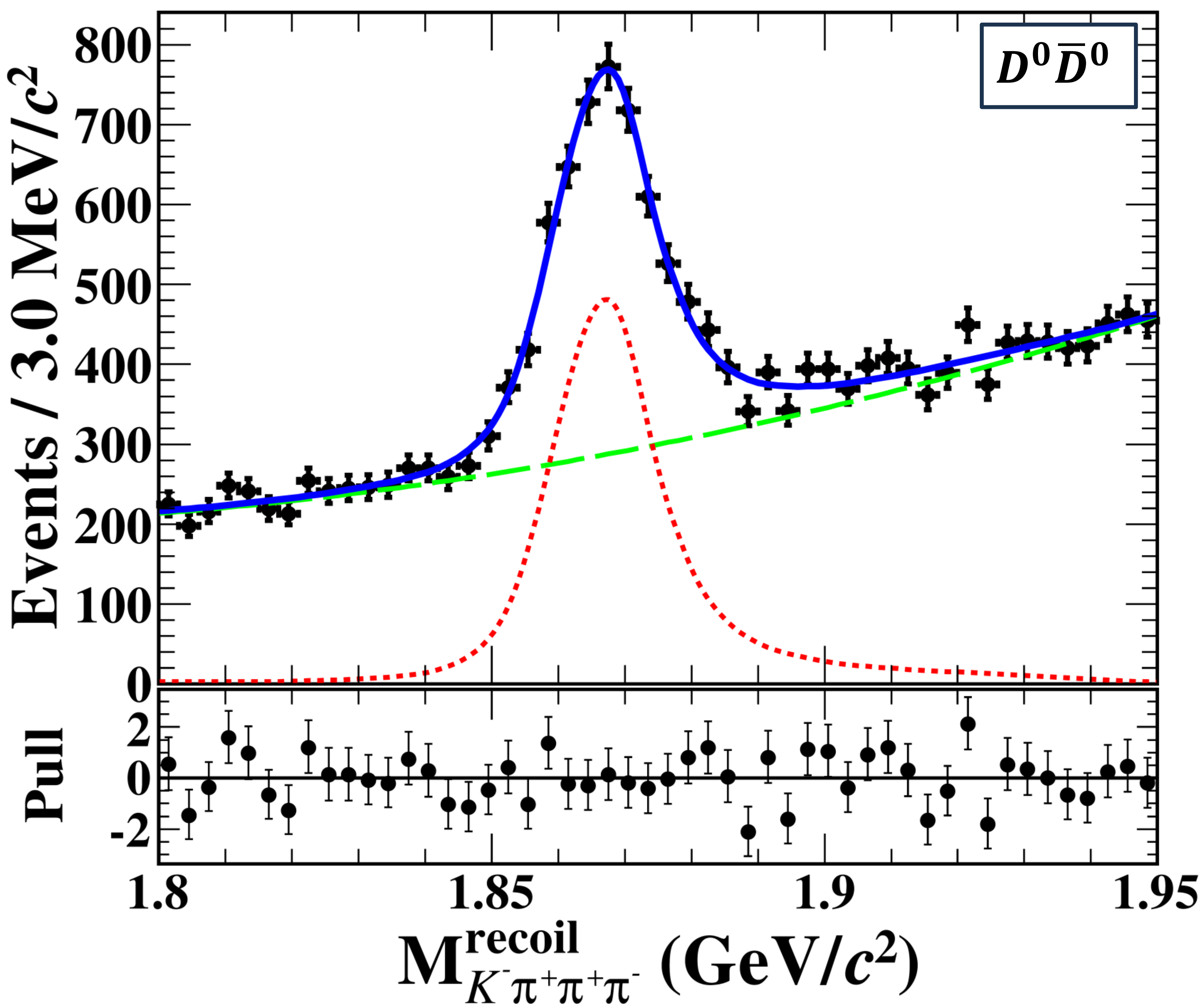

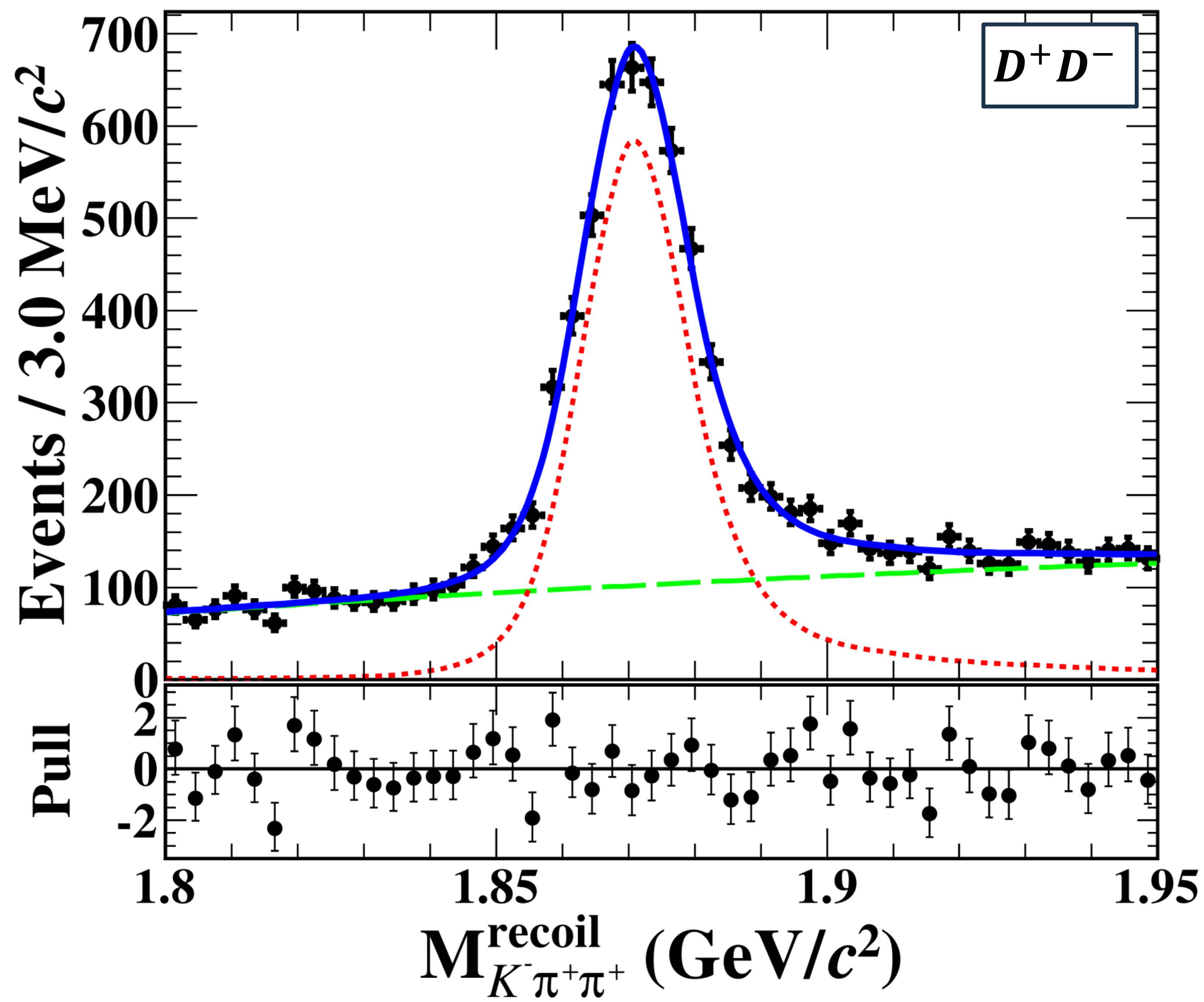

Fits to recoil mass M_D^{recoil} spectra at $\sqrt{s}$ = 4.1992 GeV; Left plot: $D^0\bar{D}^0$ **mode;** Right plot: D^+D^-**mode**

Data represented by **dots with error bars** **Fit results** indicated by **blue solid lines**

Signal shown by **red short-dashed lines** **Background** shown by **green long-dashed lines**

- Born cross section determined with

$$\sigma^B(s) = \frac{N_{\text{obs}}}{2\mathcal{L}(1+\delta)\frac{1}{|1-\prod|^2}\epsilon\mathcal{B}}$$

- Explanation the same as on slide 8th

- Simultaneous fit of dressed cross sections performed for both processes of $e^+e^- \to D^0\bar{D}^0$ and $e^+e^- \to D^+D^-$

$$\sigma^{\text{dressed}} = \sigma^B/|1-\prod|^2$$

- Parameterized as coherent sum of eight relativistic Breit-Wigner (BW) functions

$$\sigma^{\text{dressed}}(\sqrt{s}) = \left|\sum_{i=1}^{9} e^{i\phi} BW_i(\sqrt{s})\sqrt{\frac{P(\sqrt{s})}{P(M)}}\right|^2 \qquad BW(\sqrt{s}) = \frac{\sqrt{12\pi\Gamma_{ee}\mathcal{B}\Gamma}}{s-M^2+iM\Gamma}$$

  - relative phase between different BW functions -- ϕ
  - two-body phase space factor -- $P(\sqrt{s})$
  - electronic partial widths -- Γ_{ee}, decay branching fractions -- $\mathcal{B}$

- Measured Born cross sections, along with results from the CLEO-c, BaBar, and Belle
- ISR correction factor obtained through QED calculations
  - Cross sections measured in the analysis used as inputs and iterated until convergence

Cross sections of processes

$e^+e^- \to D^0\bar{D}^0$ **(top)**

$e^+e^- \to D^+D^-$ **(bottom)**

from $\sqrt{s}$ = 3.80 GeV to 4.95 GeV

Error bars include statistical and systematic uncertainties in quadrature

Comparisons shown for BESIII measurements and those from CLEO, BaBar, and Belle

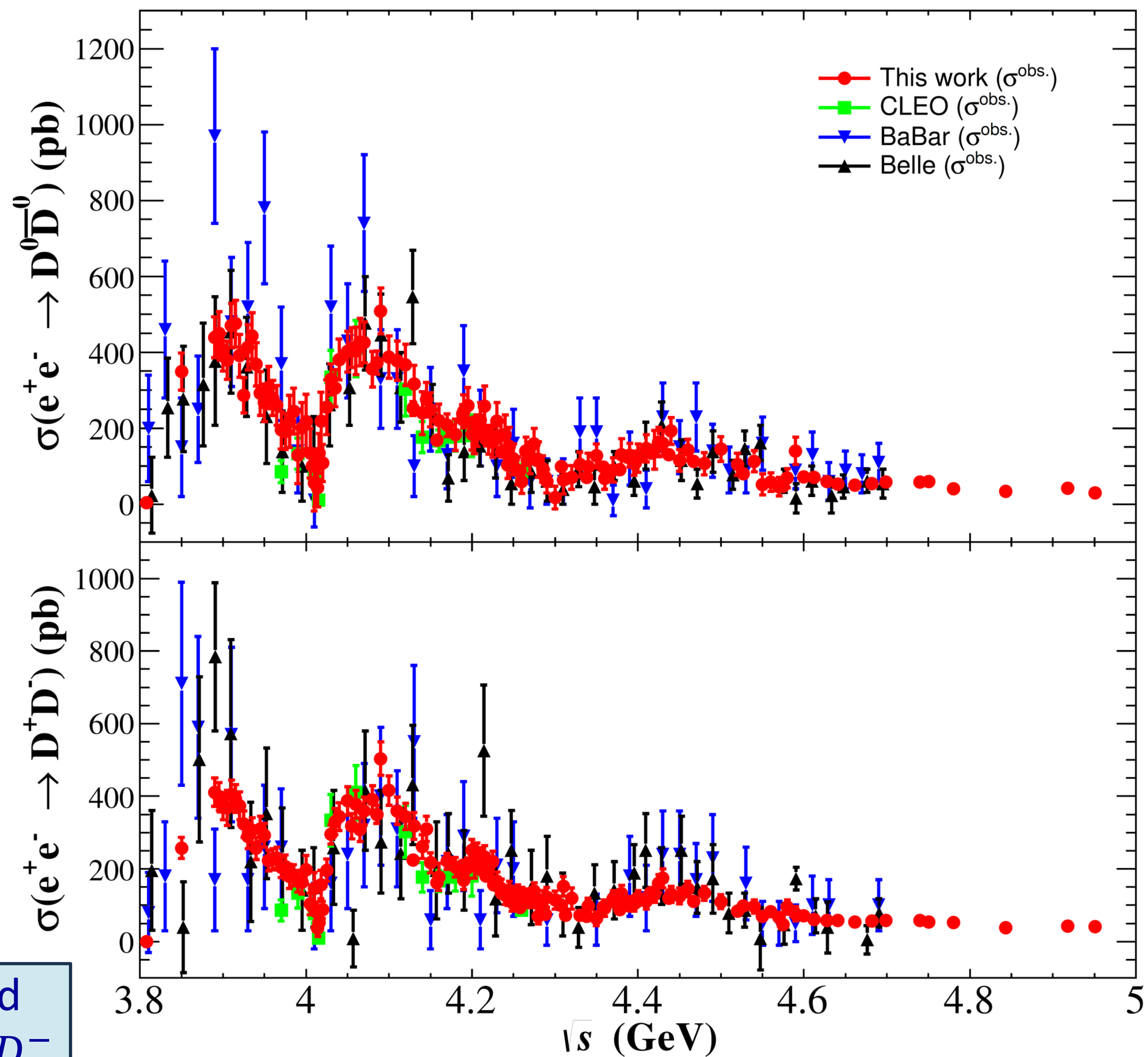

Cross-section total systematic uncertainties evaluated to be 7.0 % for $e^+e^- \to D^0\bar{D}^0$, 6.5 % for $e^+e^- \to D^+D^-$

- Good assumption of using eight resonances in simultaneous fitting from $\sqrt{s}$ = 3.80 to 4.95 GeV
- Potential new **resonance *R*** observed around 3.9 GeV with significance $> 20\sigma$

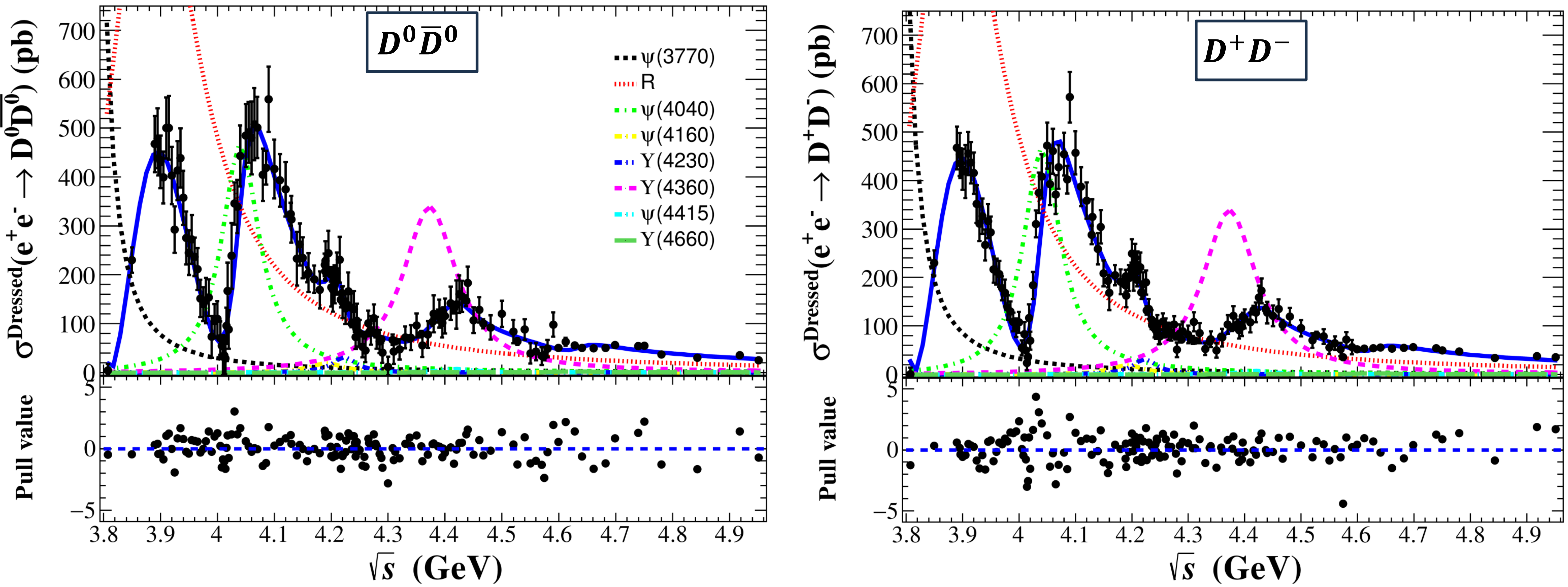

One solution of simultaneous fits to dressed cross sections for processes

$$e^+e^- \to D^0\bar{D}^0$$
$$e^+e^- \to D^+D^-$$

- However, according to

  Int. J. Mod. Phys. A 26, 4511 (2011)

  Phys. Rev. D 99, 072007 (2019)

  there should be at least 128 multiple solutions

- Also, line shape strongly model-dependent
- **Structure *R*** may be not a $c\bar{c}$ resonance
  - Threshold enhancement due to opening of $D^*\bar{D}$ channel ?
  - See arXiv:2404.03896 [hep-ph] for details

Motivation

- Looking into other processes for studying $\psi(4230)$ and $\psi(4360)$
- $\psi(4230)$ observed in processes of
  - $e^+e^- \to \pi^+\pi^- J/\psi,\ \pi^0\pi^0 J/\psi,\ K_S^0 K_S^0\, J/\psi,\ K^+K^-\, J/\psi,\ \pi^+\pi^-\psi(3686),\ \pi^+\pi^- h_c, \pi^+\pi^-\omega\chi_{c0}$
- $\psi(4360)$ observed in processes of
  - $e^+e^- \to \pi^+\pi^-\psi(3686),\ \pi^+\pi^- h_c,\ \pi^+\pi^-\psi_2(3823)$
- Similar parameters of each of these two resonances to be known (masses and widths)
  - But differences between decay modes still existing
- Updated analysis of $e^+e^- \to \eta\, J/\psi$ at 44 cm energies between 3.808 and 4.951 GeV performed by BESIII
- J/ψ and η reconstructed via
  - $J/\psi \to e^+e^-$ and $J/\psi \to \mu^+\mu^-$
  - $\eta \to \gamma\gamma$ (Mode I) and $\eta \to \pi^0\pi^+\pi^-$ (Mode II)

Top plots: Distributions of $M(l^+l^-)$ vs $M(\gamma\gamma)$ and $M(l^+l^-)$ vs $M(\pi^0\pi^+\pi^-)$; both at $\sqrt{s}$ = 4.226 GeV

Region enclosed by **red long-dashed lines** showing **signal** region
Region enclosed by **blue long-dashed lines** showing **sideband** region

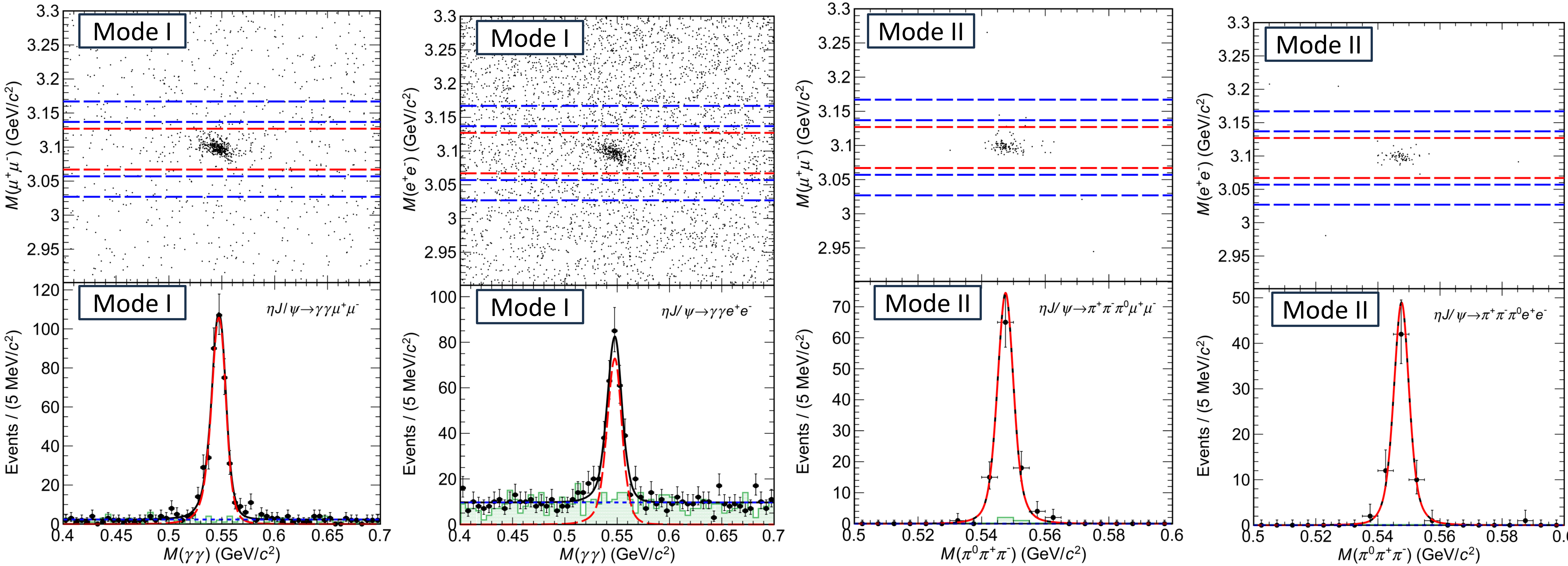

Bottom plots: Distributions of $M(\gamma\gamma)$ & $M(\pi^0\pi^+\pi^-)$ in J/ψ signal region of data sample at $\sqrt{s}$ = 4.226 GeV

Data represented by **dots with error bars** **Events from J/ψ mass sideband** given by **green histogram**

Fit result, **signal**, **background** shown by **black solid**, **red long-dashed**, **blue short-dashed lines**, respectively

- Born and dressed cross sections determined with

$$\sigma^{\mathrm{B}} = \frac{N_{\mathrm{obs}}}{\mathcal{L}_{\mathrm{int}} \cdot (1+\delta^{\mathrm{ISR}}) \cdot \frac{1}{|1-\Pi|^2} \cdot \mathcal{B} \cdot \epsilon} \qquad \sigma^{\mathrm{dressed}} = \frac{\sigma^{\mathrm{B}}}{|1-\Pi|^2}$$

- Born cross section's explanation the same as on slide 9th

- Fit function parameterized as coherent sum of three Breit-Wigner functions
  - Describing structures around 4040, 4220 and 4390 MeV, and non-resonant component

$$\sigma_{\mathrm{fit}}^{\mathrm{dressed}}(\sqrt{s}) = |\sqrt{\sigma_{NY}(\sqrt{s})} + BW_1(\sqrt{s})e^{i\phi_1} + BW_2(\sqrt{s})e^{i\phi_2} + BW_3(\sqrt{s})e^{i\phi_3}|^2$$

$$BW_i(\sqrt{s}) = \frac{\sqrt{12\pi\mathcal{B}_i\Gamma_i^{e^+e^-}\Gamma_i}}{s - M_i^2 + iM_i\Gamma_i}\sqrt{\frac{\Phi(\sqrt{s})}{\Phi(M_i)}}$$

- Non-resonant part parameterized following BaBar method

$$\Phi(\sqrt{s}) = \frac{q^3}{s} \qquad \sqrt{\sigma_{NY}(\sqrt{s})} = \sqrt{\Phi(\sqrt{s})e^{-p_0 u}p_1} \qquad u = \sqrt{s} - (M_\eta + M_{J/\psi})$$

Cross-section total systematic uncertainties = 3.8 %

- Increased statistics compared to previous BESIII measurements

Measured Born cross sections and upper limits of $e^+e^- \to \eta J/\psi$

Current BESIII measurement in good agreement with Belle and with earlier results from BESIII

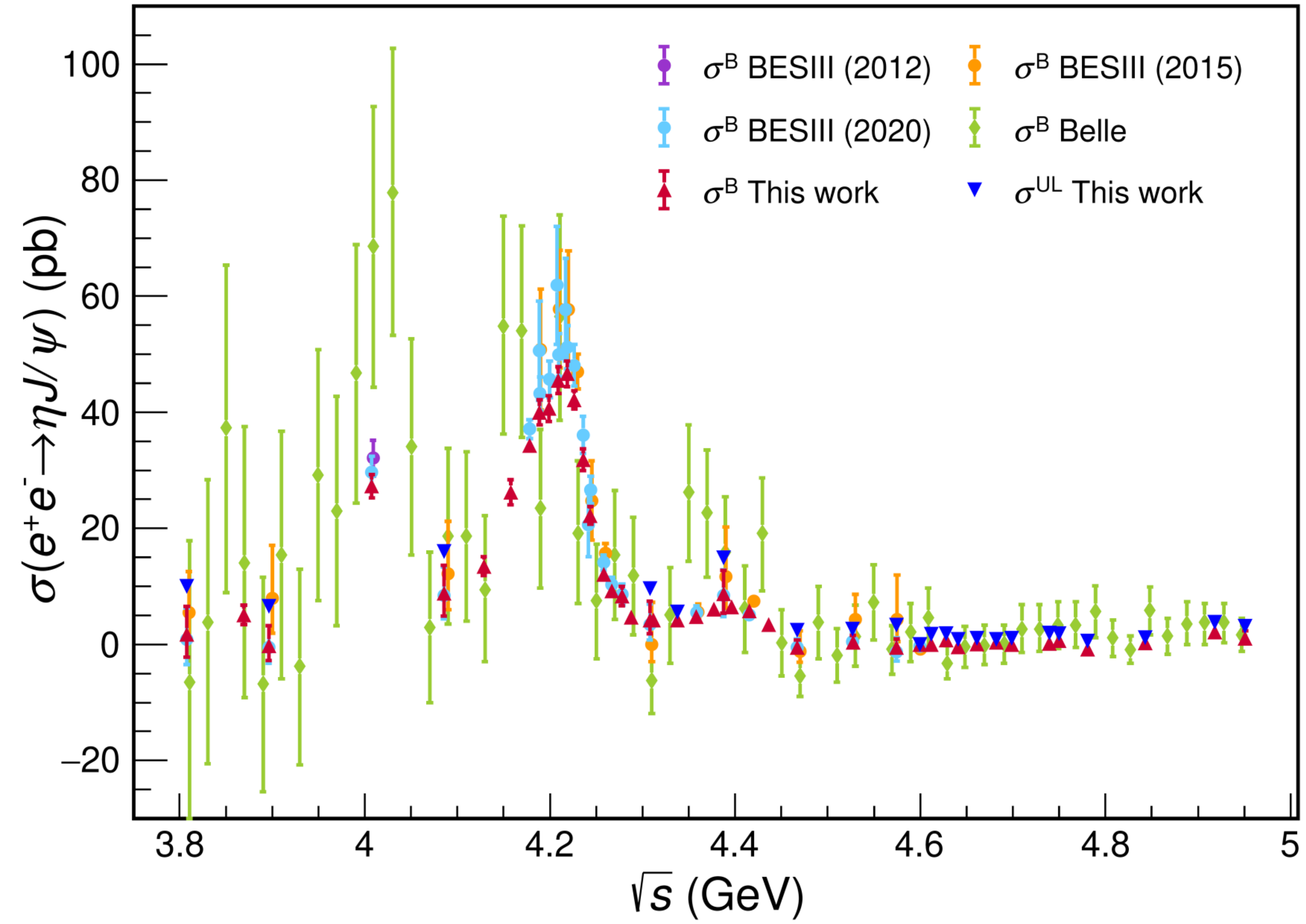

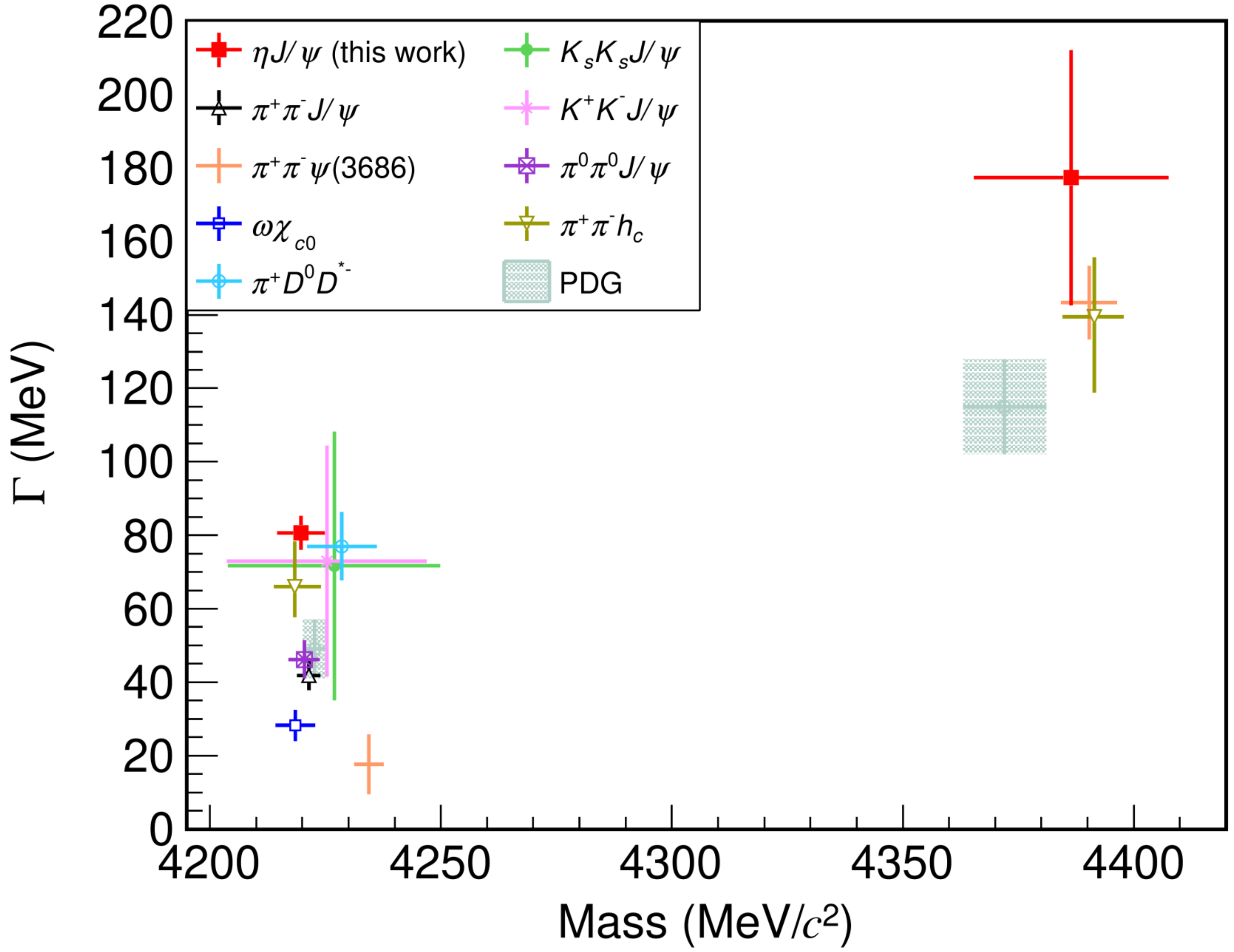

Comparison of masses vs widths of $\psi(4230)$ and $\psi(4360)$ from previous BESIII measurements and using average values in PDG

Results in bottom left are for $\boldsymbol{\psi(4230)}$

Results in top right are for $\boldsymbol{\psi(4360)}$

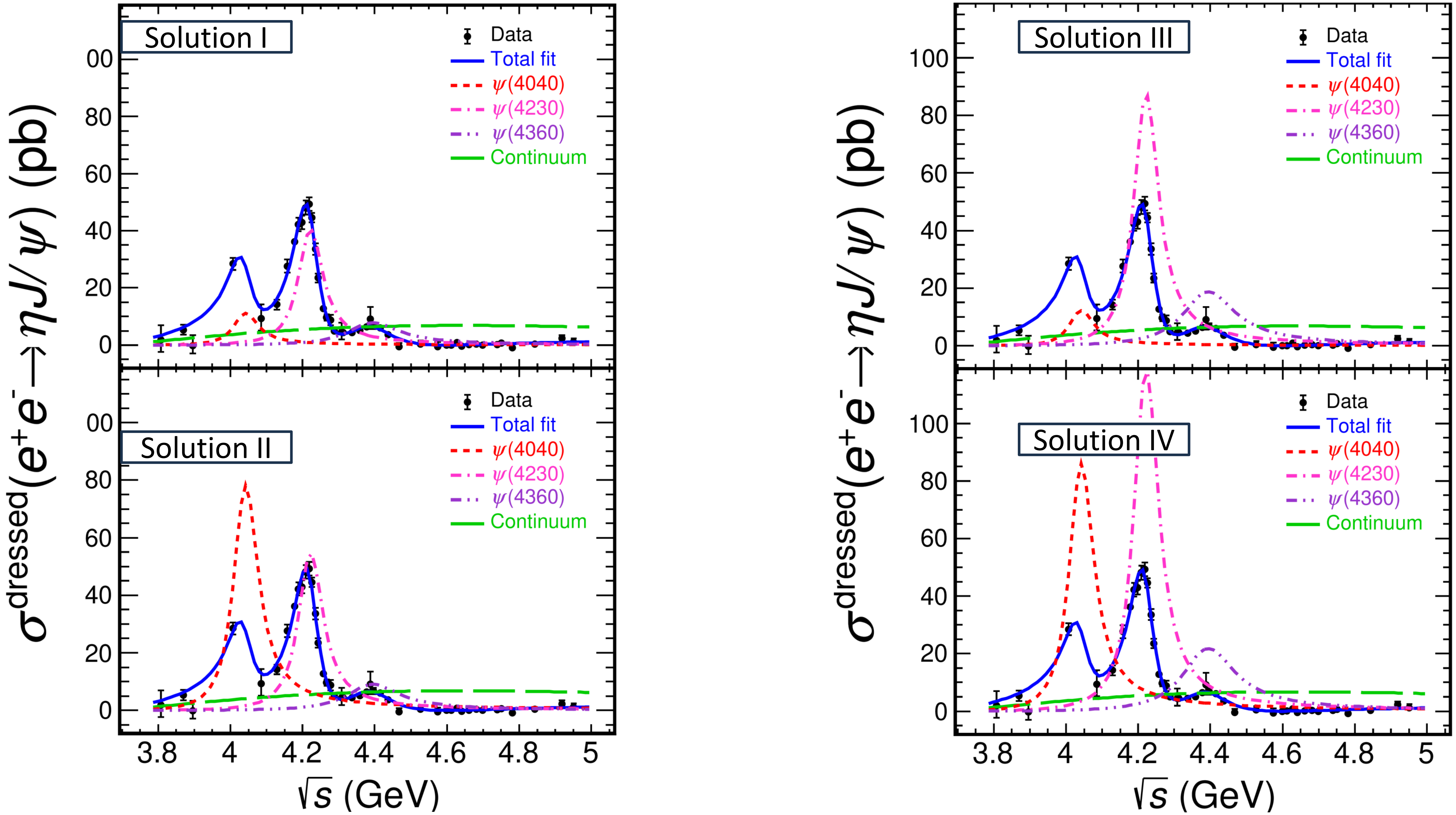

Fits to dressed cross sections of $e^+e^- \to \eta\, J/\psi$ corresponding to four solutions (see additional information to this slide in Backups)

Measured dressed cross sections given by black dots with error bars

Best fit results represented by blue solid curves with interfering amplitudes of $\psi(4040)$, $\psi(4230)$, $\psi(4360)$, and the non-resonant component

- Born cross sections of $e^+e^- \to \omega\chi_{c1,2}$ measured at cm energies from 4.308 to 4.951 GeV

- Assuming signal of $e^+e^- \to \omega\chi_{c2}$ coming from single resonance, mass and width consistent with well-established $\psi(4415)$
  - Implying existence of hidden charm decay $\psi(4415) \to \omega\chi_{c2}$

- Assuming signal of $e^+e^- \to \omega\chi_{c1}$ coming from single resonance, structure of line shape observed first time

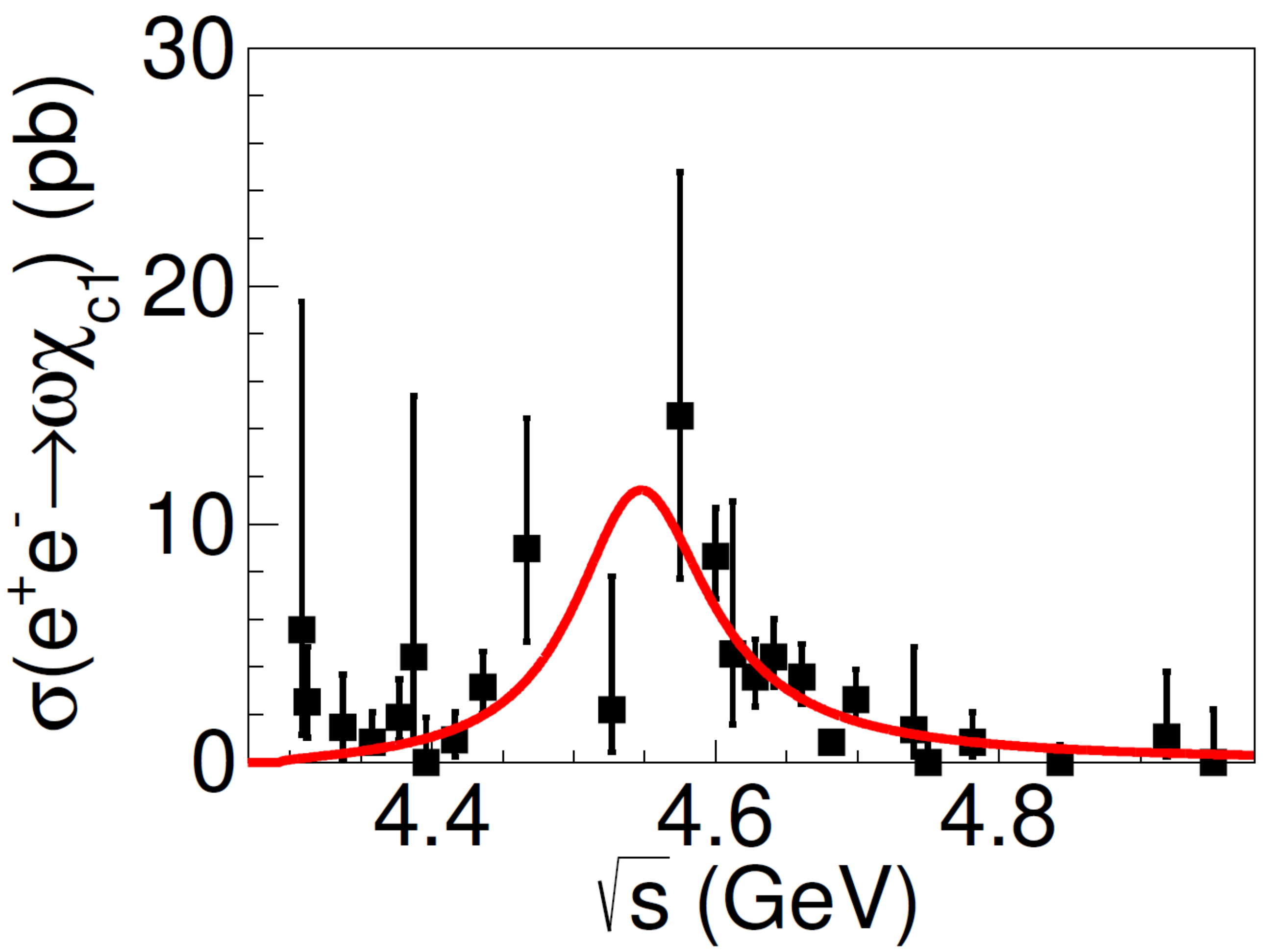

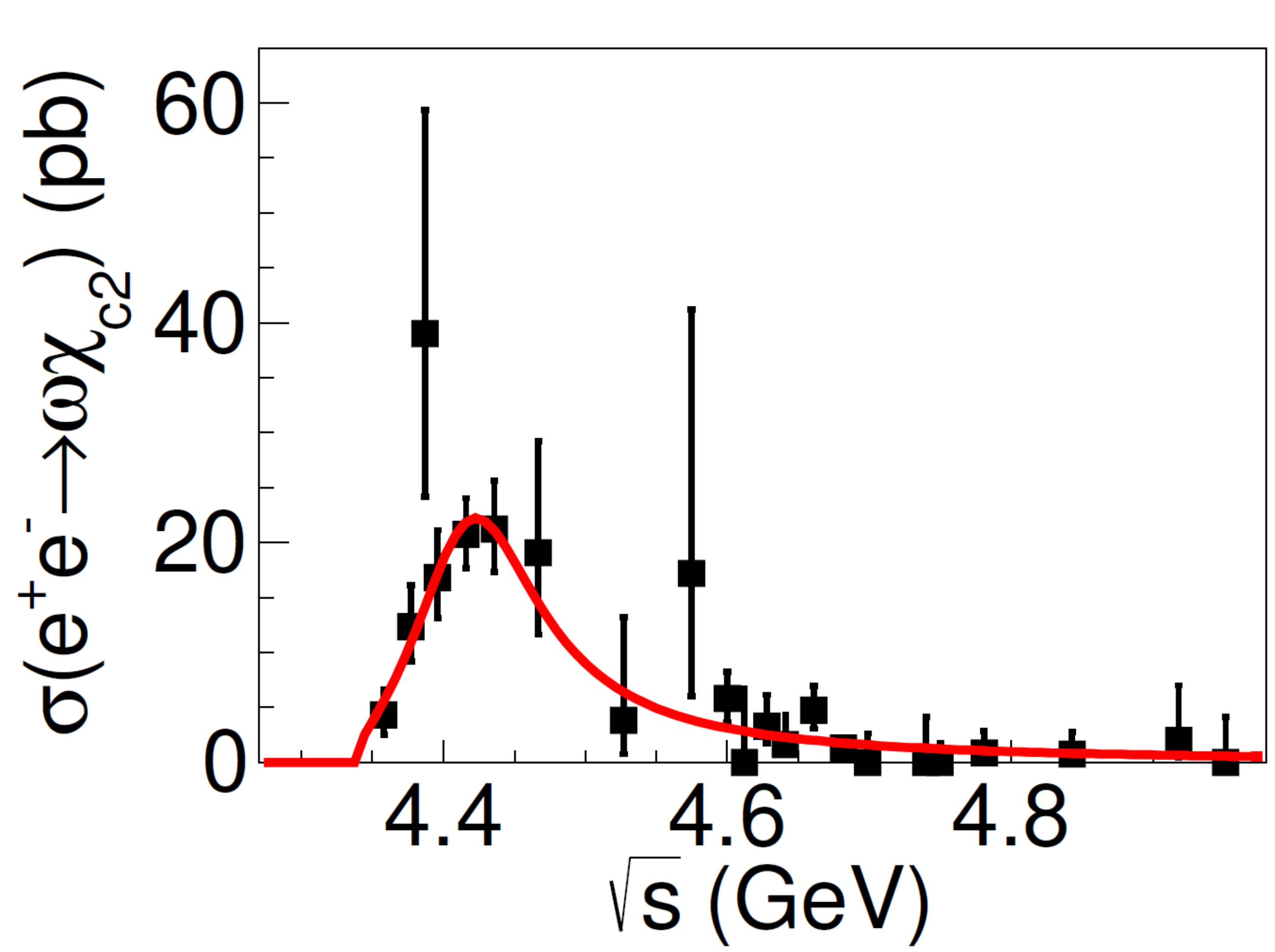

BESIII paper

Phys. Rev. Lett 132, 161901 (2024)

Observation of structures in the processes $e^+e^- \to \omega\chi_{c1}$ and $\omega\chi_{c2}$

Fits to cross sections of $e^+e^- \to \omega\chi_{c1}$ (left) and $e^+e^- \to \omega\chi_{c2}$ (right) with one single resonance

- We presented cross-section measurement results from three analyses conducted by BESIII

- Namely

1) Cross sections of $e^+e^- \to D_s^+D_s^-$
   - Several new structures observed in cross-section line shape
   - Giving important input for coupled-channel analyses and theoretical model testing

2) Cross sections of $e^+e^- \to D\bar{D}$
   - Here also, interesting structures observed in cross-section line shape
   - Critical for deeper understanding of non-conventional/conventional states in given energy range

3) Cross sections of $e^+e^- \to \eta\, J/\psi$
   - Mass and width of measured two states consistent with those of previously measured $\psi(4230)$ and $\psi(4360)$
   - Providing more precisely studied line shape than before

Thanks !

Backups

- Understanding strong interaction dynamics through a way provided by hadron spectroscopy
- Experimental data playing important role on various theoretical models
- Abundance of XYZ states existing with charm and bottom quark content
- Properties of XYZ do not fit to heavy quarkonium spectrum
- Majority of these states observed in e^+e^- collisions and heavy hadron decays, like in
  - BES, BESII and BESIII experiments
  - Belle and Belle II experiments
  - CLEO and BaBar experiments
- Explore other production mechanisms as well, such as in electron-proton scattering in
  - COMPASS-II, JLab experiments and EIC

- Detector cylindrical core covering 93% of the full solid angle and consisting of
  - helium-based multilayer drift chamber (MDC)
  - plastic scintillator time-of-flight system (TOF)
  - CsI(Tl) electromagnetic calorimeter (EMC)
  - all enclosed in a superconducting solenoidal magnet providing a 1.0 T magnetic field
- EMC measuring photon energies
  - with a resolution of 2.5% at 1 GeV in the barrel region
  - with a resolution of 5% at 1 GeV in the end cap region
- TOF time resolution
  - 68 ps in the barrel region
  - 110 ps in the end cap region
- End cap TOF system upgraded in 2015 to provide 60 ps resolution

- BESIII detector's geometric description and detector's response included GEANT4-based MC simulation software packages (BOOST & EVTGEN)

- Beam energy spread and initial-state radiation (ISR) in e^+e^- annihilation simulated and modeled by KKMC program

- Combined TOF and dE/dx information used to perform PID

- Charge particle final-state radiation (FSR) incorporated with PHOTOS package

- Charged track candidates reconstructed from hits in multilayer drift chamber (MDC)
  - polar angle to satisfy $\cos\theta < 0.93$
  - point of closest approach to e^+e^- interaction vertex to be within ± 10 cm in beam direction as well as within 1 cm in the plane perpendicular to the beam direction

- Signal MC samples used to determine reconstruction efficiencies, ISR correction factors and vacuum polarization (VP)

Fit results to Born cross section

S symbolizing statistical significance

First uncertainties are statistical, second uncertainties are systematic

$e^+e^- \to D\bar{D}$								
Resonance	$\psi(3770)$	R	$\psi(4040)$	$\psi(4160)$	$Y(4230)$	$Y(4360)$	$\psi(4415)$	$Y(4660)$
Mass (MeV/c^2)	3773.7 (fixed)	3872.5±14.2±3.0	4039 (fixed)	4191 (fixed)	4222.5 (fixed)	4374 (fixed)	4421 (fixed)	4630 (fixed)
Width (MeV/c^2)	87.6 (fixed)	179.7±14.1±7.0	80 (fixed)	70 (fixed)	48 (fixed)	118 (fixed)	62 (fixed)	72 (fixed)
$\Gamma_{ee}\mathcal{B}$ (eV)	95-106	202-292	41-44	1-2	1-2	50-144	0-2	0-1
S(σ)	10	> 20	13	7	11	11	4	8
χ^2/d.o.f $= 346/275$				p-value = 0.002				

Fit results to $e^+e^- \to \eta J/\psi$ cross sections, with given fit parameters M_i, Γ_i, $\Gamma_i^{e^+e^-}$, B_i, and ϕ_i

Label i = 1, 2 and 3 symbolizing $\psi(4040)$, $\psi(4230)$, and $\psi(4360)$, respective

Only statistical uncertainties shown

Parameter	Solution I	Solution II	Solution III	Solution IV
M_1 (MeV/c^2)	4039 (fixed)			
Γ_1 (MeV)	80 (fixed)			
$\Gamma_1^{e^+e^-} \cdot \mathcal{B}_1$ (eV)	1.0 ± 0.2	7.1 ± 0.6	1.1 ± 0.2	7.8 ± 0.6
M_2 (MeV/c^2)	4219.7 ± 2.5			
Γ_2 (MeV)	80.7 ± 4.4			
$\Gamma_2^{e^+e^-} \cdot \mathcal{B}_2$ (eV)	4.0 ± 0.5	5.5 ± 0.7	8.7 ± 1.0	11.9 ± 1.1
M_3 (MeV/c^2)	4386.4 ± 12.6			
Γ_3 (MeV)	176.9 ± 32.1			
$\Gamma_3^{e^+e^-} \cdot \mathcal{B}_3$ (eV)	1.8 ± 0.6	2.1 ± 0.7	4.3 ± 1.3	5.0 ± 1.5
ϕ_1 (rad)	3.1 ± 0.6	-1.8 ± 0.1	3.3 ± 0.4	-1.6 ± 0.1
ϕ_2 (rad)	-2.8 ± 0.1	2.9 ± 0.2	-2.0 ± 0.1	-2.6 ± 0.2
ϕ_3 (rad)	-2.9 ± 0.1	3.0 ± 0.1	2.8 ± 0.1	2.4 ± 0.7
p_0 (MeV^{-1})	1.5 ± 0.4	1.5 ± 0.4	1.5 ± 0.4	1.6 ± 0.4
p_1 (GeV^{-3})	390.0 ± 155.3	389.3 ± 155.6	389.5 ± 155.1	389.5 ± 154.5